Cellulose (2019) 26:1895–1908
https://doi.org/10.1007/s10570-018-2182-8

ORIGINAL RESEARCH

Dexamethasone-containing bioactive dressing for possible application in post-operative keloid therapy

Agnieszka Rojewska · Anna Karewicz · Marta Baster · Mateusz Zając · Karol Wolski · Mariusz Kępczyński · Szczepan Zapotoczny · Krzysztof Szczubiałka · Maria Nowakowska

Received: 17 August 2018 / Accepted: 6 December 2018 / Published online: 10 December 2018

Abstract Bioactive dressing based on bacterial cellulose modified with carboxymethyl groups (mBC) was successfully prepared and studied. The surface of mBC was activated using carbodiimide chemistry and decorated with alginate/hydroxypropyl cellulose submicroparticles containing dexamethasone phosphate (DEX-P). Prior to their deposition particles were coated with chitosan in order to facilitate their binding to mBC, and to increase the control over the release process. The detailed physicochemical characterization of the particles and the bioactive dressing was performed, including the determination of the particles' size and size distribution, DEX-P encapsulation efficiency and loading, particles' distribution on the surface of the mBC membrane, as well as DEX-P release profiles from free and mBC-bound particles. Finally, the preliminary cytotoxicity studies were performed. The fabricated bioactive material releases DEX-P in a controlled manner for as long as 25 h. Biological tests in vitro indicated that the dexamethasone-containing submicroparticles are not toxic toward fibroblasts, while effectively inhibiting their proliferation. The prepared bioactive dressing may be applied in the treatment of the post-operative wounds in the therapy of keloids and in other fibrosis-related therapies.

A. Rojewska · A. Karewicz (✉) · M. Baster · M. Zając · K. Wolski · M. Kępczyński · S. Zapotoczny · K. Szczubiałka · M. Nowakowska
Faculty of Chemistry, Jagiellonian University in Kraków, Gronostajowa 2, 30-387 Kraków, Poland
e-mail: a.rojewska@doctoral.uj.edu.pl

A. Karewicz
e-mail: karewicz@chemia.uj.edu.pl

M. Baster
e-mail: marta.baster@gmail.com

M. Zając
e-mail: m91.zajac@doctoral.uj.edu.pl

K. Wolski
e-mail: wolski@chemia.uj.edu.pl

M. Kępczyński
e-mail: kepczyns@chemia.uj.edu.pl

S. Zapotoczny
e-mail: zapotocz@chemia.uj.edu.pl

K. Szczubiałka
e-mail: szczubia@chemia.uj.edu.pl

M. Nowakowska
e-mail: nowakows@chemia.uj.edu.pl

Graphical abstract

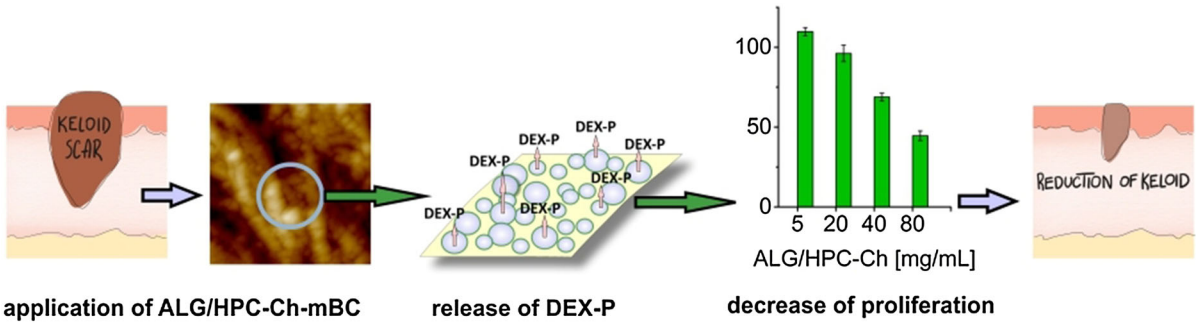

Keywords Alginate · Hydroxypropyl cellulose · Dexamethasone phosphate · Modified bacterial cellulose · Wound healing · Drug release

Introduction

Dexamethasone sodium phosphate (DEX-P) is a water-soluble derivative of dexamethasone (DEX), a potent corticosteroid used widely to treat various inflammatory and autoimmune conditions. Although many pharmaceutical applications of DEX-P are based on its anti-inflammatory activity (Hickey et al. 2002; Zhang et al. 2016; Hu et al. 2017), its use as a bioactive component of the implants, stents and wound dressings can also benefit from the anti-proliferative (Bao et al. 2016) and anti-apoptotic properties of the drug toward fibroblasts (Nieuwenhuis et al. 2010). DEX and DEX-P were shown to have a negative influence on wound healing process, but only when administered systemically for longer time periods, in particular when the patient was treated with that drug prior to injury (Wang et al. 2013). No significant influence of the short-term post injury/surgery application of DEX and DEX-P was, however, confirmed so far. On the contrary, there are reports on the positive effects of DEX in healing process. DEX was applied with success in repair of the mucous membrane defects in oral submucous fibrosis (Raghavendra Reddy et al. 2012). In that study Reddy et al. have used DEX-impregnated collagen membranes to cover the raw wound created by surgical excision of fibrous bands. The presence of the drug was shown to decrease the inflammatory reaction and extent of the fibrosis process, most probably due to the reduced proliferation and deposition of fibroblasts. Beule et al. (2009) have shown the ability of DEX to decrease postoperative osteogenesis in a standardized animal wound model for endoscopic surgery of sinus. Li et al. (2014) have recently proposed the electrospun polymer fiber meshes based on poly(lactide-co-glycolide) (PLGA) as a delivery vehicle for DEX and green tea polyphenols. The obtained, bioactive dressing was proposed for the post-operative therapy of keloids. Hydrophilic green tea polyphenols were introduced as necessary permeation enhancers for hydrophobic DEX, simultaneously providing antibacterial activity.

The long-term systemic treatment with DEX may lead to various adverse effects, including swelling, insomnia, bleeding of the stomach or intestines, Cushing's Syndrome, diabetes, or osteoporosis (Vardy et al. 2006; Ren et al. 2015). The systemic absorption of the topically administered DEX is low, but not negligible (Weijtens et al. 2002). Thus, there is a need for a controlled delivery system for DEX-P. In response to this challenge, we have developed a nanoparticulate delivery system for DEX-P based on the alginate-hydroxypropylcellulose (ALG/HPC) composite. Such system can be utilized in various topical applications to increase the duration, efficiency and safety of therapy. In a current paper we used that system as a component of a bioactive dressing. For that purpose the obtained ALG/HPC particles containing DEX-P were coated with a thin layer of chitosan to increase the control over the drug release and enable their binding to bacterial cellulose (Bionanocellulose®, BC). They were then covalently bound to the modified Bionanocellulose® membrane (mBC), which was obtained by functionalization of BC with carboxyl groups. BC was chosen because it

constitutes an excellent wound dressing (Ul-Islam 2013; Liu 2016). It is a natural biopolymer material consisting of the interconnected network of cellulose fibrils. BC has high surface area and high ability for water retention. Due to its high sorption ability it allows to remove exudates from the wound, while providing the moist environment which promotes healing processes and prevents the formation of scars (Moritz et al. 2014; Napavichayanun et al. 2016). Ionically-modified BC was shown to have a better stability in water and higher water retention (Spaic 2014).

The studies presented in the current paper were carried out based on the hypothesis that one can fabricate the bioactive wound dressing material by immobilization on the surface of BC the polysaccharide submicroparticles containing dexamethasone phosphate (ensuring prolonged and controlled release profile of that drug) which can be particularly useful in the therapy of post-operative wounds, especially those resulting from the surgical treatment of the pathologies related to the uncontrolled proliferation of the fibrous tissue (fibrosis, keloid).

Experimental part

Materials

The sheets of Bionanocellulose® modified with carboxymethyl groups (mBC) were kindly provided by Biovico company [(6.07 ± 0.42) nmol of carboxylic groups per 1 mm^2 of mBC surface (Guzdek et al. 2018)]. Dexamethasone 21-phosphate disodium salt (DEX-P, ≥ 98%, Sigma-Aldrich), hydroxypropyl cellulose (HPC, M_W = 100,000 g/mol, Sigma-Aldrich), alginic acid sodium salt (ALG, medium molecular weight, from brown algae, Sigma-Aldrich; M_v = 260,000 g/mol, M/G ratio = 1.20), chitosan (low molecular weight, Sigma-Aldrich, M_v = 120,000 g/mol, degree of deacetylation DDA = 79%), calcium chloride (p.a., Fluka, Poland), 1-ethyl-3-(3-dimethylaminopropyl)carbodiimide (EDC, Sigma-Aldrich, commercial grade, powder), *N*-hydroxysuccinimide (NHS, 98%, Sigma-Aldrich), 2-propanol (99.9% pure, Sigma Aldrich), acetonitrile (gradient grade for liquid chromatography, Sigma-Aldrich), acetic acid (≥ 99.5%, Chempur), fluorescein sodium salt (powder, Sigma Aldrich), rhodamine B isothiocyanate (powder, Sigma-Aldrich), sodium phosphate monobasic dihydrate (≥ 99.0%, Sigma-Aldrich) were used as received. Dulbecco's Modified Eagle's Medium–high glucose (DMEM), phosphate buffered saline tablets (PBS) and Cell Proliferation Kit II (XTT) were purchased from Sigma-Aldrich; HyClone Research Grade Fetal Bovine Serum, South American Origin (FBS), HyClone trypsin–EDTA and HyClone Penicillin–Streptomycin solution were purchased from Symbios.

Synthesis of ALG/HPC submicroparticles containing DEX-P

To encapsulate DEX-P into the nanospheres, 20 mg of the drug was dissolved in 5 mL of water. Then 50 mg of sodium alginate (ALG) and 12.5 mg of hydroxypropyl cellulose (HPC) were dissolved in this solution. After stirring for 1 h at room temperature, the resulting solution was injected at 0.05 mL/min with a syringe pump (Aladdin-1000, World Precision Instruments) to a solution of cross-linking agent (0.2 M calcium chloride, 10 mL) under continuous stirring. The obtained ALG/HPC particles were filtered off using a fritted glass funnel (11-G4), washed with distilled water and isopropanol and dried at room temperature.

Coating ALG/HPC particles with chitosan

20 mg of nanospheres was added to 1 mL of 1% (w/v) solution of chitosan in 1% (w/v) acetic acid and stirred at room temperature for 2 h. The excess of the chitosan was then removed by filtration on a Büchner funnel (11-G4) and the obtained ALG/HPC-Ch particles were dried at room temperature.

Deposition of ALG/HPC-Ch on BC modified with carboxyl groups (mBC)

To attach the chitosan-coated nanospheres on the surface of nanocellulose modified with carboxyl groups, a 4 cm^2 sheet of mBC was immersed in an acetate buffer (pH 5.5) at room temperature. NHS (0.025 M) and EDC (0.008 M) were then added sequentially and the sample was continuously

stirred at 150 rpm for 120 min. The activated BC was rinsed with deionized water, incubated with the suspension of the nanospheres (100 mg) in phosphate buffer (pH 7.4) for 30 min, and washed thoroughly with deionized water. The deposition reaction was carried out in the ultrasound bath to prevent aggregation of the particles. The obtained samples of mBC with attached particles (ALG/HPC-Ch-mBC) were dried in the air.

Release profiles: entrapment efficiency and loading capacity determination

20 mg of the ALG/HPC particles loaded with DEX-P was placed in a 15 mL centrifuge tube and 5 mL of 10 mM PBS (pH 7.4) was added. The sample was incubated at 37 °C (IKA, a KS 3000 incubator) with continuous agitation (140 rpm). After defined time intervals the sample was centrifugated at 10,000 rpm for 5 min and then the supernatant was collected. The new portion (5 mL) of PBS was added to the nanospheres and the system was placed back in the incubator. The experiment was performed in four repetitions.

To study the release profiles of DEX-P from ALG/HPC-Ch-mBC, a 4 cm^2 sample of ALG/HPC-Ch-mBC was incubated in 5 mL of 10 mM PBS (pH 7.4). The sample was incubated at 37 °C with continuous agitation (140 rpm). After defined time intervals the supernatant was collected, replaced with the new portion (5 mL) of PBS and the system was placed back in the incubator. The experiment was performed in four repetitions.

The concentration of DEX-P in the collected samples was determined using an HPLC system (Waters) consisting of a 515 pump, a rheodyne-type dosing system and a 2996 Photodiode Array Detector. The separation was performed on a C18 column (3.9 mm × 150 mm, 5 μm), using a 30:70 (v/v) mixture of acetonitrile and 10 mM phosphate buffer (pH 7.4) as the mobile phase at a flow rate of 0.5 mL/min. The drug signal was detected at 241 nm (absorption maximum of DEX-P). All the measurements were done in triplicate. DEX-P concentration was calculated based on the calibration curve obtained for the standard solutions (R^2 = 0.999). Entrapment efficiency (EE [%]) and loading capacity (LC [%]) were calculated based on the total amount of the drug released from the obtained particles, using the following equations:

$$EE[\%] = \frac{Total\ weight\ of\ DEX - P\ in\ the\ obtained\ submicroparticles}{Weight\ of\ DEX - P\ used\ in\ the\ synthesis} \times 100 \quad (1)$$

$$LC\,[\%] = \frac{Weight\ of\ DEX - P\ encapsulated\ in\ the\ sample}{Weight\ of\ the\ sample} \times 100 \quad (2)$$

Microscopic and spectroscopic characterization of the unbound and mBC-bound particles

SEM analysis was carried out using a PhenomWorld Pro scanning electron microscope. ALG/HPC-Ch spheres were dried at room temperature on a watch glass, and then the obtained material was placed on a carbon tape. The mBC membrane with the attached particles was stretched flat on a glass slide, dried in vacuum and placed on a carbon tape. Atomic force microscopic (AFM) images were obtained using a Dimension Icon AFM microscope (Bruker, Santa Barbara, CA) working in the PeakForce Tapping (PFT) and QNM® modes with standard silicon cantilevers for measurements in the air (nominal spring constant of 0.4 N/m).

For confocal laser scanning microscopy (CLSM) studies the mBC membranes were stained with the aqueous solution of fluorescein sodium salt (0.1 mg/mL) for 72 h before the particle deposition. Chitosan-coated particles were also labeled with rhodamine B isothiocyanate (0.1 mg/mL solution) in 0.1 M phosphate buffer (pH 9.0) 24 h prior to the deposition on mBC. The deposition was carried out as previously described. Images were acquired using an A1-Si Nikon (Japan) confocal laser scanning system built on a Nikon inverted microscope Ti-E using a Plan Apo 100×/1.4 Oil DIC objective. Diode lasers (488 nm and 561 nm) were used for excitation.

FTIR spectra were recorded using a Nicolet iS10 FT-IR spectrometer equipped with an ATR accessory (SMART iTX).

Cytotoxicity studies

Cell culture

Mouse Embryonic Fibroblasts MEF ATCC SCRC-1008 (MEFs) were maintained in a cell culture dish containing DMEM with streptomycin (100 μg/mL) and penicillin (100 U/mL) supplemented with 5% (v/v) FBS. The cells were incubated at 37 °C, 90% humidity with 5% CO_2. Before toxicity and proliferation assessment, the cells (at approximately 70% confluence) were washed twice with PBS solution and subsequently harvested after 3 min incubation with 1 mL of 0.25% trypsin with 0.1% EDTA. After adding 3 mL of DMEM [with 5% (v/v) FBS] the cell suspension was centrifugated at 1250 g for 5 min, the supernatant was removed, and the pellet was resuspended in DMEM and 5% (v/v) FBS.

Toxicity and proliferation

MEFs suspended in DMEM supplemented with 5% (v/v) FBS were seeded into a 48-well cell culture plate (0.5 mL) at 5.2×10^4 (cytotoxicity) or 2.5×10^4 (proliferation) cells/well and incubated (37 °C, 5% CO_2, 90% humidity). After 8 h (proliferation) or 29 h (cytotoxicity) the medium was replaced with 0.5 mL of fresh DMEM (supplemented with 5% (v/v) FBS in the case of proliferation test) containing different nanospheres concentration. After 23.5 h (cytotoxicity) or 42 h (proliferation) XTT assay was performed. It is based on reduction of tetrazolium salt XTT to formazan salt which occurs only in metabolically active (live) cells. The medium was removed and 200 μL of fresh DMEM with 100 μL of the activated XTT mixture was added to each well [with 5% (v/v) FBS in a final solution in the case of proliferation test]. After 2.5 h of incubation the plate was analyzed using a microplate reader (EPOCH2, Biotek Instruments, Inc) by measuring the absorbance at 460 nm. The results are normalized to an untreated control (without the nanospheres). All the data were presented as the mean of three replicates with standard deviation of the mean.

Results and discussion

Low solubility of DEX in water (85 mg/L) (Messner and Loftsson 2010) limits its application as a component of the wound-healing dressings, as these are supposed to provide moist environment and are often based on hydrogels. On the other hand, DEX-P has similar anti-inflammatory and immunosuppressive properties, while showing higher solubility in aqueous media, thus it can be successfully introduced into the hydrogel matrix. To ensure the control over the release of DEX-P we have encapsulated it into the nanoparticulate system based on natural polysaccharides, and then used these particles to modify the surface of mBC.

Encapsulation of DEX-P in ALG/HPC particles

The initial experiments allowed us to select the optimal composition of the ALG/HPC hydrogel matrix of the particles, which in the case of DEX-P was found to be 4:1 w/w. We have shown previously that this particular hydrogel composition can be used to encapsulate bioactive macromolecules [heparin (Karewicz et al. 2010)] and alkaline phosphatase (Karewicz et al. 2014). The DEX-P containing submicroparticles were obtained using the extrusion technique. Their diameter was maintained at an average value of 170 nm by adjusting the injection rate of the polymeric mixture containing the active agent into the solution of cross-linking agent (0.2 M $CaCl_2$) and the flow of the inert gas, which was applied parallel to the injection flow.

Figure 1a shows a typical SEM image of the particles produced using the method described above. They were spherical in shape and showed moderate tendency to aggregate. The dispersity of the obtained particles was significant, which is a typical outcome of the extrusion method. However, the diameter of 96% of particles did not exceed 500 nm, with the average diameter of 175 nm. The histogram showing the distribution of sizes of the obtained particles is presented in Fig. 1b.

Coating ALP/HPC particles with chitosan

To facilitate the attachment of the DEX-P-loaded particles to the surface of mBC via EDC/NHS chemistry, as well as to increase the control over the

release profile, the nanospheres were coated with a thin layer of chitosan using polycation-polyanion electrostatic interactions. The chitosan-coated particles (ALG/HPC-Ch) retained the spherical shape and did not significantly change their average size as illustrated by the SEM image (Fig. 2). The diameter of 96% of the chitosan-coated particles did not exceed 600 nm, with the average diameter of 190 nm. Due to the fact that the coating process was carried out in an aqueous solution, the drug loss was unavoidable and it was estimated that ca. 18% of the initially loaded drug was lost. The concentration of the drug released from the ALG/HPC-Ch particles was, however, still at the desired therapeutic level (Dayanarayana et al. 2014).

Release profiles of DEX-P from ALG/HPC and ALG/HPC-Ch particles

Release profiles of DEX-P from the submicroparticles were studied under physiological conditions (PBS, pH 7.4, 37 °C). Each experiment was conducted fourfold, and each collected supernatant was measured in triplicate. Figure 3 shows a typical chromatogram (panel A) and the release profiles (panel B). 50% of DEX-P was released from the uncoated submicroparticles within the first 45 min and from the particles coated with chitosan within the first 75 min. In both systems the drug was still being released after 24 h.

Based on the total amount of DEX-P released from the submicroparticles, the encapsulation efficiency (EE) and loading capacity (LC) were calculated for both uncoated and chitosan-coated particles. The obtained EE and LC values for uncoated particles were found to be (65.1 ± 1.1)% and (14.9 ± 0.6)%, respectively. For the chitosan coated particles these values were slightly lower: (53.0 ± 1.9)% and (12.2 ± 1.7)%, respectively. EE was satisfactory for both systems, and LC was comparable or higher than that obtained for DEX-P in other micro/nanoparticulate systems described in literature (Jaraswekin et al. 2007).

Deposition of ALG/HPC-Ch particles on mBC

The ALG/HPC/Ch submicroparticles containing DEX-P were covalently attached to the surface of Bionanocellulose® modified with carboxymethyl groups (mBC) using EDC/NHS methodology. The coupling reaction led to the formation of amide bonds between the amino groups of chitosan and the carboxyl groups of mBC. To avoid the use of an excess of the coupling agents, the concentrations of EDC and NHS necessary for activation of carboxymethyl groups were first optimized. In order to minimize the release of DEX-P from the nanospheres during their binding to mBC, the shortest required exposure time to the coupling agents solution was also established. The optimal concentrations and exposure time were found based on the changes in the amount of the particles bound to mBC and DEX-P released from the mBC modified with nanospheres (Table 1). To estimate the weight of attached particles, the weight of particles remaining in the solution after the deposition process was determined. The concentration of DEX-P was measured with HPLC in the same conditions as in the release profile experiments. In all experiments EDC:NHS ratio was 1:3.

The optimal time of mBC exposure to coupling agents was established first and was found to be 2 h. It enabled effective attachment of particles (19.93 ± 0.10 mg of particles/cm^2) and the highest amount of drug released from mBC (2.15 ± 0.15 mg/cm^2). The amount of attached particles decreased only slightly with decreasing concentration of EDC and NHS therefore the amount of both compounds could be significantly reduced while maintaining an effective attachment of the nanospheres to mBC. A fourfold reduction of EDC and NHS concentrations (to 0.008 M and 0.025 M, respectively) allowed to remove any detectable (based on HPLC analysis) traces of coupling agents from the material by washing with small amount of water, without any significant reduction in the amount of entrapped DEX-P.

To confirm the formation of amide bonds, the FTIR-ATR spectra of the unmodified mBC sheets, ALG/HPC-Ch and ALG/HPC-Ch-mBC were measured (Fig. 4). The covalent attachment of the particles to the mBC surface was confirmed by the presence of the strong amide band I (at 1644 cm^{-1}, stretching vibrations of C=O group of amide bond) and amide band II (1561 cm^{-1}, deforming vibrations of N–H group of amide bond) in the sample of ALG/HPC-Ch-mBC

The morphology of the ALG/HPC-Ch-mBC material was visualized using SEM, AFM and confocal microscopy. SEM images revealed the presence of a large amount of nanometric spherical structures at the surface of mBC (Fig. 5). SEM images of the surface of pristine mBC and the surface of mBC with attached

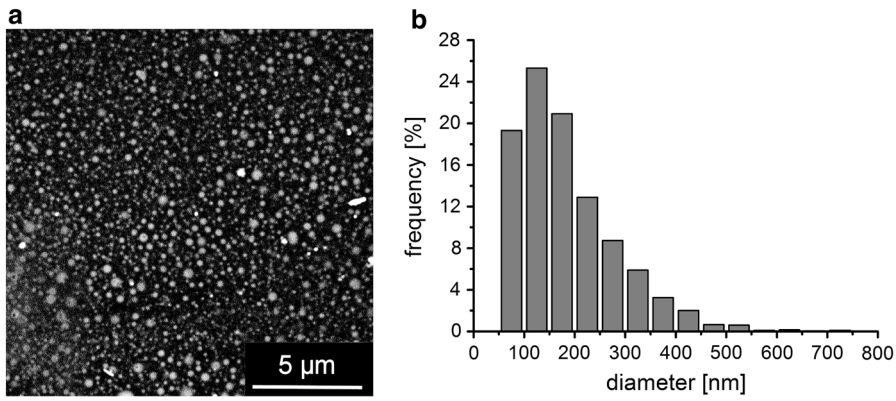

Fig. 1 **a** SEM analysis of the uncoated ALG/HPC particles with DEX-P, **b** histogram showing size distribution of ALG/HPC particles

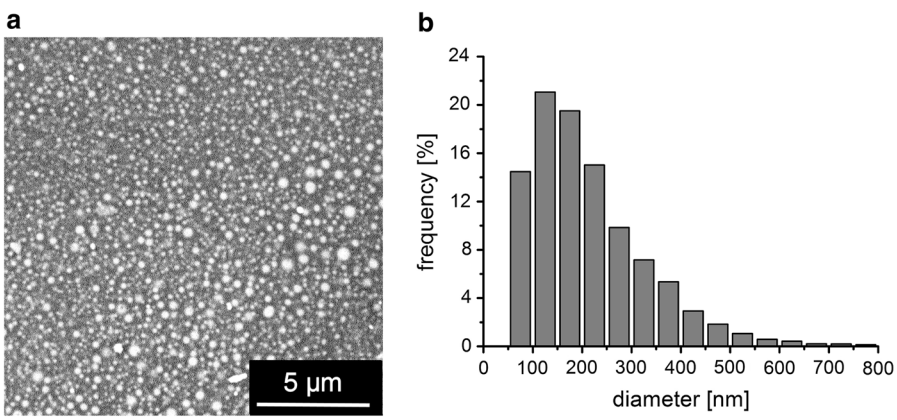

Fig. 2 **a** SEM image of chitosan-coated particles (ALG/HPC-Ch) containing encapsulated DEX-P, **b** histogram showing size distribution of ALG/HPC-Ch with DEX-P

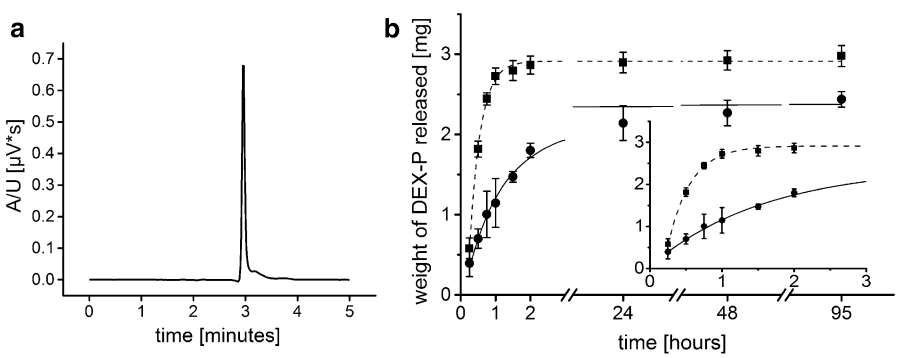

Fig. 3 **a** Typical chromatogram of DEX-P released under physiological conditions (37 °C, pH 7.4) from the uncoated ALG/HPC particles containing DEX-P, **b** The release profiles of DEX-P from the uncoated ALG/HPC particles (squares) and particles coated with chitosan (circles)

ALG/HPC-Ch particles are shown in Fig. 5a, b. The comparison of the histograms presented on Figs. 2b and 5c leads to the conclusion that the smaller submicroparticles are preferentially attached to mBC.

This observation was confirmed using the AFM visualization. The results of the AFM measurements are presented in Fig. 6. The strands of submicroparticles decorating nanocellulose fibrils are clearly visible. The analysis of the AFM images allows to define the average size of the attached particles as being around 100–120 nm, which is in a good agreement with the SEM analysis. It should be

Table 1 Optimization of the mBC activation procedure with EDC and NHS as coupling agents

Time of exposure to EDC/NHS (h)	Concentration of EDC (mol/L)	Concentration of NHS (mol/L)	DEX-P released from attached particles (mg/cm^2)	Weight of attached particles (mg/cm^2)
1	0.050	0.150	0.63 ± 0.08	5.75 ± 0.07
2	0.050	0.150	2.15 ± 0.15	19.93 ± 0.10
3	0.050	0.150	1.98 ± 0.20	18.38 ± 0.03
5	0.050	0.150	1.30 ± 0.13	12.13 ± 0.04
24	0.050	0.150	1.15 ± 0.25	10.70 ± 0.03
2	0.050	0.150	2.15 ± 0.15	19.93 ± 0.10
2	0.025	0.075	2.08 ± 0.05	14.88 ± 0.44
2	0.012	0.037	2.05 ± 0.03	14.70 ± 0.31
2	0.008	0.025	1.95 ± 0.10	13.85 ± 0.34
2	0.004	0.012	1.03 ± 0.05	7.40 ± 0.11

stressed, that due to the significant pressure of the tip exerted on the soft hydrogel particle, the AFM images do not represent well the shape of the particle, thus the diameter can be reasonably estimated only in the horizontal direction.

The confocal microscopy was used to study the extent to which the particles penetrate the 3D structure of the mBC sheet. The mBC fibrils and DEX-P-loaded particles were fluorescently labeled with fluorescein sodium salt and rhodamine B isothiocyanate (green and red fluorescence), respectively. The 3D image (Fig. 7a) shows a spatial distribution of the ALG/HPC-Ch particles in mBC. Most of the submicroparticles occupy the surface or the space close to the surface of mBC, however, small number of particles was distributed evenly in the whole volume of the mBC sheet. Therefore, although most of the drug would be released form the surface, a small amount of DEX-P will diffuse slowly through the nanocellulose hydrogel to reach the contact with the wound much later, thus possibly prolonging the healing effect of the material. The 2D image (Fig. 7b) shows the surface of mBC with particles distributed alongside the cellulose nanofibrils.

Release of DEX-P from ALG/HPC-Ch-mBC hydrogel material

The release of DEX-P from the mBC-attached submicroparticles was studied. The drug was released

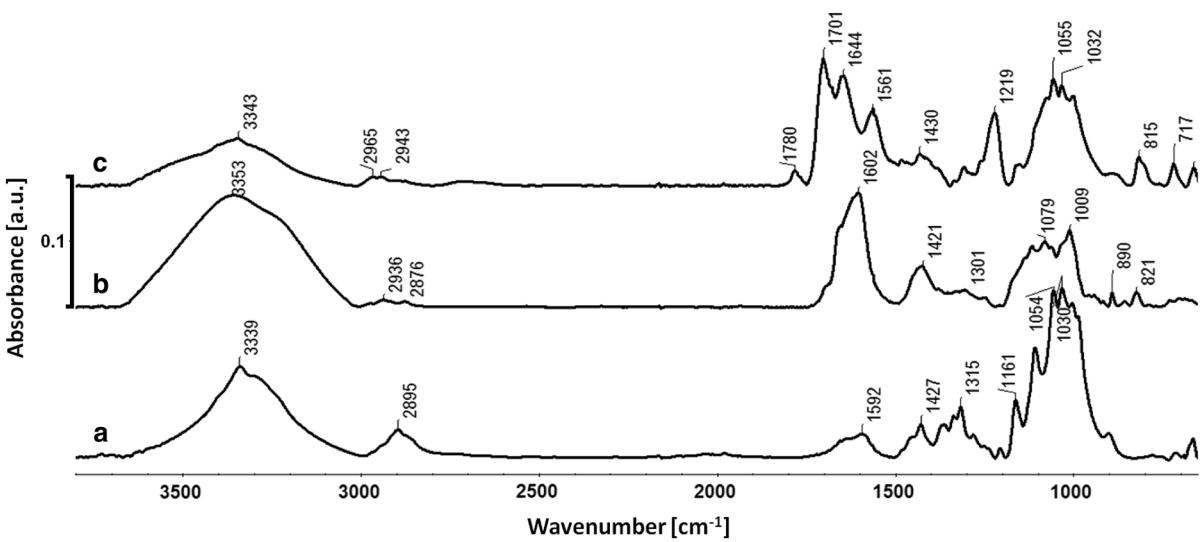

Fig. 4 FTIR-ATR spectra of (a) mBC, (b) ALG/HPC-Ch, and (c) ALG/HPC-Ch-mBC

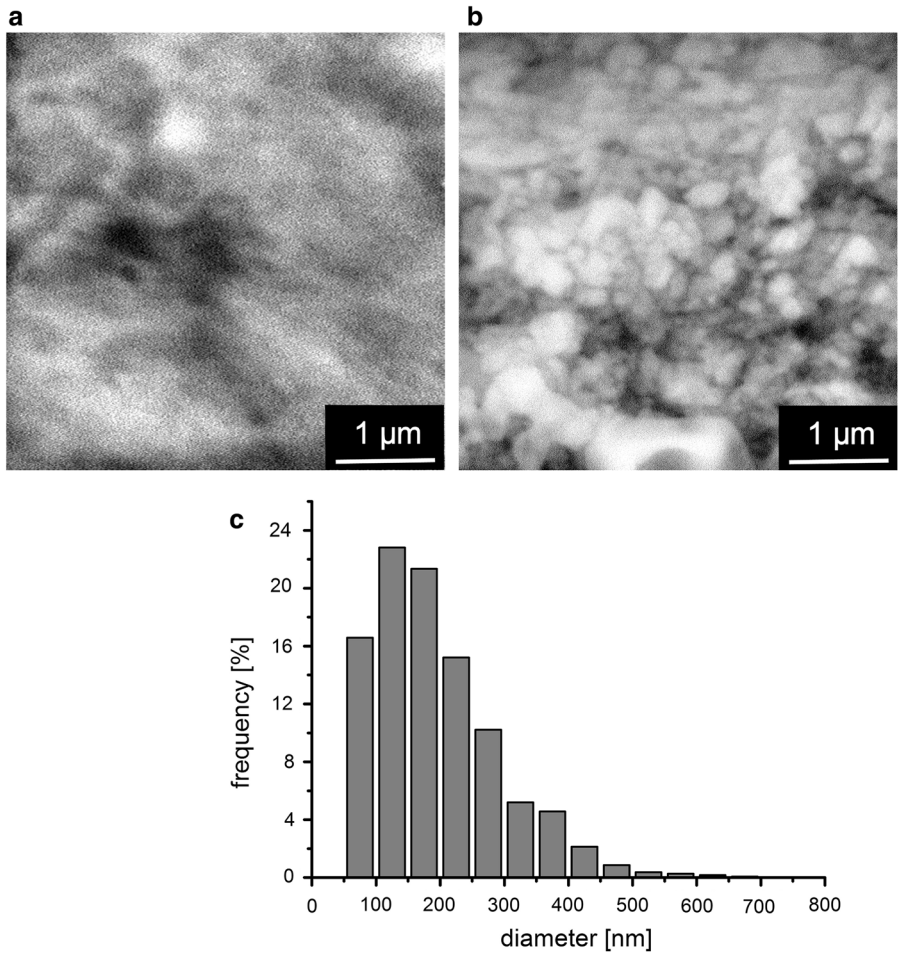

Fig. 5 **a** SEM image of mBC, **b** SEM image of ALG/HPC-Ch-mBC, **c** histogram showing size distribution of ALG/HPC-Ch bound to the surface of mBC

from the material in a controlled manner, as shown in Fig. 8. The release profile is advantageous, with fast release during the first few hours, and slow but still significant delivery of DEX-P for up to 2 days. A separate experiment was also designed to confirm the beneficial impact of the encapsulation of DEX-P in the submicroparticles attached to the mBC hydrogel matrix on the resulting release profile. For this purpose mBC was incubated in 0.75 mg/mL solution of DEX-P in PBS for 1 h in order to allow its diffusion into the material. The release profile of the free drug entrapped physically in mBC was then studied. The obtained profile (Fig. 8) was characterized by undesirable "burst release" and all the entrapped drug was released within 2 h. That confirms that our approach involving entrapment of DEX-P in the mBC hydrogel matrix is reasonable.

We attempted to fit different kinetic models, frequently applied to the drug release from the nano/microparticulate systems, to our data in order to obtain some insight into the possible release mechanism. The fitting parameters obtained for the three models used (Higuchi, Peppas and Weibull) are presented in Table 2. The Higuchi model resulted in the relatively poor approximation for all of the obtained systems, thus it was not taken into consideration in further analysis. Fitting the experimental data to the Peppas model gave the highest R^2 values for both: unbound and m-BC-bound chitosan-coated particles, therefore it was used as the best model for the release from the proposed dressing. It also gave a relatively good fit for

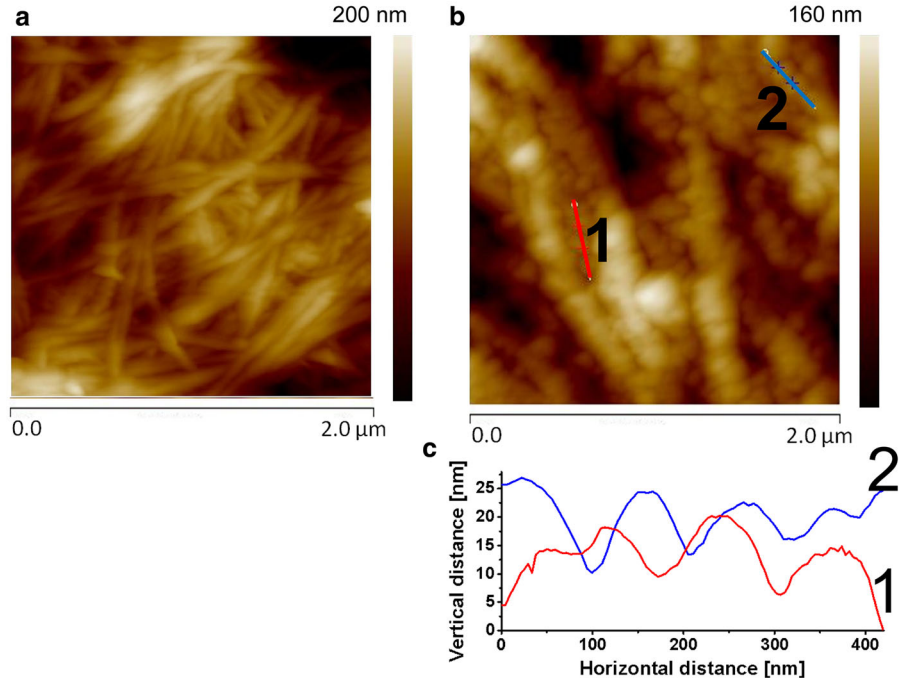

Fig. 6 **a** AFM image of mBC, **b** AFM image of ALG/HPC-Ch-mBC material containing DEX-P, **c** AFM cross-section profiles marked as 1 and 2 in the image **b**

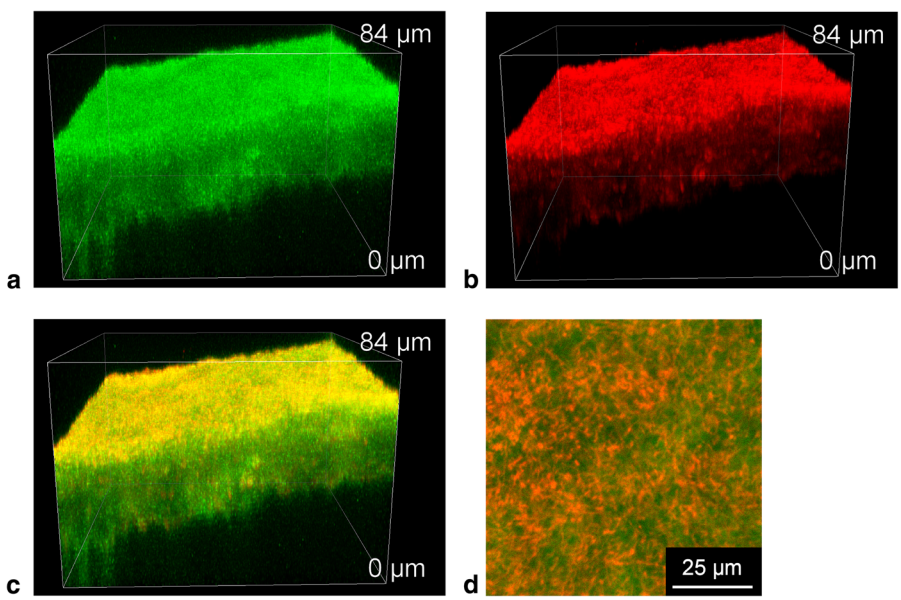

Fig. 7 Confocal microscopy images of the mBC labelled with fluorescein after the deposition of rhodamine B-labelled ALG/HPC-Ch submicroparticles containing DEX-P: **a** 3D image in the green channel (FITC), **b** 3D image in the red channel (rhodamine B), **c** 3D image showing a merge of green and red channels, **d** 2D image of the sample—merge of green and red channels. (Color figure online)

uncoated particles, as illustrated in Fig. 9. This model is a short time approximation, so the fitting procedure has to be limited to the first 60% of the release profile. In this semi-empirical equation a is the kinetic constant and k is an exponent characterizing the diffusion mechanism. For uncoated particles the release exponent k suggested that the drug release was driven by a Fickian diffusion from the spherical matrix, whereas for coated particles and mBC attached particles a non-Fickian diffusion is the most possible release mechanism. The empirical Weibull model allows to take into consideration the whole data set. Depending on the correlation between the d value in the Weibull equation and the type of diffusional

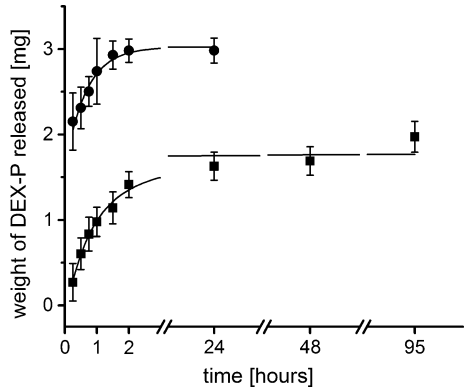

Fig. 8 Release profiles of DEX-P from ALG/HPC-Ch-mBC (squares) and from mBC pre-incubated in a PBS solution of free DEX-P (0.75 mg/mL) (circles)

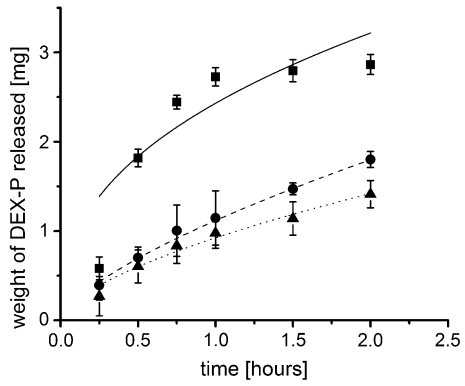

Fig. 9 Release data fits to Peppas model for ALG/HPC particles (squares), ALG/HPC-Ch particles (circles) and mBC bound ALG/HPC-Ch particles (triangles)

Table 2 Parameters obtained by fitting different release kinetic models to experimental release profiles for uncoated, chitosan-coated and mBC-bound particles

System	Uncoated submicroparticles	Unbound chitosan-coated submicroparticles	mBC with attached chitosan-coated submicroparticles
Higuchi $y = a\sqrt{x}$			
a	2.41	1.21	0.96
R^2	0.695	0.953	0.947
Peppas $y = ax^k$			
a	2.43	1.12	0.92
k	0.41	0.69	0.62
R^2	0.731	0.998	0.976
Weibull $y = a - (a - b)e^{(-kx)^d}$			
a	0.520	2.36	1.72
b	2.92	0.23	0
k	2.41	0.61	0.92
d	− 2.57	1.23	0.87
R^2	0.998	0.989	0.931

mechanism of drug release one can specify the type of release from the obtained particles (Papadopoulou et al. 2006). For the uncoated particles *d* was found to be 0.75, which suggests that Fickian diffusion in either fractal or Euclidian spaces is dominant. For mBC with attached submicroparticles *d* is in the range of 0.75–1, which is typical for a combined (Fickian diffusion and Case II transport) mechanism. For chitosan-coated particles *d* is higher than 1, suggesting more complex release mechanism. In all cases the Peppas model analysis leads to the conclusions which are in agreement with these obtained based on the Weibull model.

Biological studies—cell viability and proliferation

Nanocellulose is well known to be highly biocompatible and non-toxic (Lin and Dufresne 2014). To verify whether the ALG/HPC-Ch submicroparticles generate any toxic effect to fibroblasts, the cell viability assay was performed. Figure 10a shows that at the concentrations up to 20 mg/mL the empty ALG/HPC-Ch submicroparticles (carrier) caused no toxicity to the mouse embryonic fibroblasts (MEFs), while for the DEX-P-loaded particles only slight toxicity was observed, with cell viability in the range of 80–95%. At higher ALG/HPC-Ch concentrations (40 and 80 mg/mL) some toxicity of the carrier was registered for empty particles (still the viability was above 70%), whereas the protective effect of DEX-P was revealed. This is in agreement with some previous reports where the protective effect of DEX on various cell lines, including endothelial cells (Zakkar et al. 2011) and fibroblasts (Mendoza-Milla et al. 2005) was observed. These results and no significant fibroblast necrosis suggest the DEX-containing dressing is safe. This is essential, as the healthy tissue on the edges of the wound may be in contact with the dressing. It is also important for the wound itself, as necrosis may increase inflammatory response (Davidovich et al. 2014), resulting in the elevated pro-fibrotic activity (White and Mantovani 2013). In attempt to assess the influence of the DEX-P-loaded ALG/HPC-Ch on the proliferation of fibroblasts the suitable proliferation

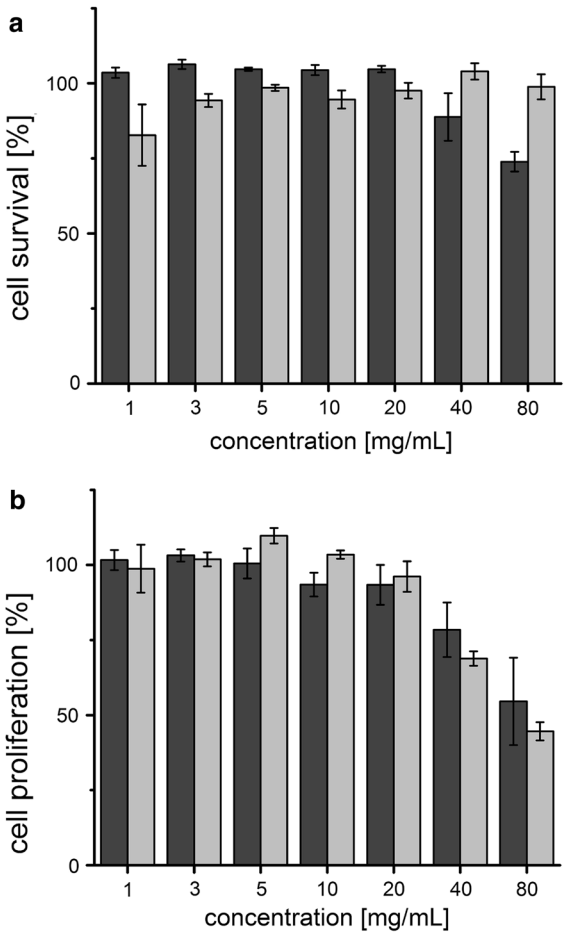

Fig. 10 **a** MEF cell viability test results, **b** MEF cell proliferation test results (black—empty particles, grey—DEX-P-loaded particles)

test was also performed (Fig. 10b). The proliferation was not hindered by neither empty nor loaded submicroparticles at the concentration below 10 mg/mL. Although DEX-P has positively influenced the proliferation observed for the loaded ALG/HPC-Ch in the concentration range of 10–20 mg/mL, at higher concentrations the inhibition effect of both: the carrier and the drug on the proliferation rate is clearly visible. The inhibitory effect was more pronounced for DEX-P containing submicroparticles, as expected (Wu et al. 2006). One can conclude that the DEX-P-loaded submicroparticles at concentrations equal or higher than 40 mg/mL can effectively inhibit fibroblast proliferation. As shown before, 40 mg of DEX-P-loaded submicroparticles is deposited on ca. 5 cm^2 of the ALG/HPC-Ch-mBC surface, although it can be also observed, that the material will contain relatively limited amount of water and will be in direct contact with the wound. This may lead to higher DEX-P concentrations and a satisfactory decrease in proliferation rate even at considerably lower surface of contact.

Conclusions

DEX-P was successfully encapsulated in the ALG/HPC submicroparticles. These particles were then surface-modified with chitosan to obtain ALG/HPC-Ch system. Both ALG/HPC and ALG/HPC-Ch particles showed spherical morphology, high DEX-P encapsulation efficiency (65.1% and 53%, respectively) and drug loading values, which were comparable to other delivery systems for DEX-P. A thin layer of chitosan coating increased the control over the DEX-P release profile and allowed to covalently attach ALG/HPC-Ch particles to mBC. DEX-P was released from the particles attached to mBC in a controlled manner for up to 2 days. Additional experiments confirmed the advantage of DEX-P encapsulation in submicroparticles prior to introduction into mBC matrix over the direct introduction of the drug into mBC matrix. Preliminary biological studies showed that no toxicity is induced by both empty and DEX-P-loaded submicroparticles up to 20 mg/mL and only a slight decrease in fibroblasts viability at the concentration up to 80 mg/mL could be observed. At the concentration above 40 mg/mL the DEX-P-loaded particles have effectively inhibited proliferation of fibroblasts.

Based on the results of our studies we can conclude that we have successfully fabricated the novel bioactive wound dressing material combining the advantageous properties of BC and these of dexamethasone. Due to the decoration of BC surface with submicroparticles containing encapsulated DEX-P the drug release from the material could be controlled, ensuring its local concentration at the required therapeutic level (e.g. that needed to inhibit the fibroblasts proliferation).

In view of the negligible cytotoxicity combined with anti-inflammatory properties and ability to inhibit fibroblast proliferation the proposed system may constitute a promising bioactive dressing useful for the treatment of the wound fibrosis.

Acknowledgments Authors would like to thank The National Centre for Research and Development (NCBiR) for the financial support in the form of grant no. K/NCB/000013 obtained in the frame of the INNOTECH Programme. The research was carried out with the equipment purchased thanks to the financial support of the European Regional Development Fund in the framework of the Polish Innovation Economy Operational Programme (Contract No. POIG.02.01.00-12-023/08). Karol Wolski would like to thank the Fundation for Polish Science for the financial support (START 96.2018).

Compliance with ethical standards

Conflict of interest The authors declare that they have no conflict of interest.

References

Bao Z, Gao P, Xia G, Wang Z, Kong M, Feng Ch, Cheng X, Liu Y, Chen X (2016) A thermosensitive hydroxybutyl chitosan hydrogel as a potential co-delivery matrix for drugs on keloid inhibition. J Mater Chem B 4:3936–3944. https://doi.org/10.1039/C6TB00378H

Beule AG, Steinmeier E, Kaftan H, Biebler KE, Gopferich A, Wolf E, Hosemann W (2009) Effects of a dexamethasone-releasing stent on osteoneogenesis in a rabbit model. Am J Rhinol Allergy 23:433–436. https://doi.org/10.2500/ajra.2009.23.3331

Davidovich P, Kearney CJ, Martin SJ (2014) Inflammatory outcomes of apoptosis, necrosis and necroptosis. Biol Chem 395:1163–1171. https://doi.org/10.1515/hsz-2014-0164

Dayanarayana U, Doggalli N, Patil K, Shankar J, Sanjay MKP (2014) Non surgical approaches in treatment of OSF. IOSR-JDMS 13:63–69. https://doi.org/10.9790/0853-131136369

Guzdek K, Lewandowska-Łańcucka J, Zapotoczny S, Nowakowska M (2018) Novel bionanocellulose based membrane protected with covalently bounded thin silicone layer as promising wound dressing material. Appl Surf Sci 459:80–85. https://doi.org/10.1016/j.apsusc.2018.07.180

Hickey T, Kreutzer D, Burgess DJ, Moussy F (2002) Dexamethasone/PLGA microspheres for continuous delivery of an anti-inflammatory drug for implantable medical devices. Biomaterials 23:1649–1656. https://doi.org/10.1016/S0142-9612(01)00291-5

Hu J-B, Kang X-Q, Liang J, Wang X-J, Xu X-L, Yang P, Ying X-Y, Jiang S-P, Du Y-Z (2017) E-selectin-targeted sialic acid-PEG-dexamethasone micelles for enhanced anti-inflammatory efficacy for acute kidney injury. Theranostics 7:2204–2219. https://doi.org/10.7150/thno.19571

Jaraswekin S, Prakongpan S, Bodmeier R (2007) Effect of poly(lactide-co-glycolide) molecular weight on the release of dexamethasone sodium phosphate from microparticles. J Microencapsul 24:117–128. https://doi.org/10.1080/02652040701233655

Karewicz A, Zasada K, Szczubiałka K, Zapotoczny S, Lach R, Nowakowska M (2010) "Smart" alginate-hydroxypropylcellulose microbeads for controlled release of heparin. Int J Pharm 385:163–169. https://doi.org/10.1016/j.ijpharm.2009.10.021

Karewicz A, Zasada K, Bielska D, Douglas TEL, Jansen JA, Leeuwenburgh SCG, Nowakowska M (2014) Alginate-hydroxypropylcellulose hydrogel microbeads for alkaline phosphatase encapsulation. J Microencapsul 31:68–76. https://doi.org/10.3109/02652048.2013.805841

Li J, Fu R, Li L, Yang G, Ding S, Zhong Z, Zhou S (2014) Co-delivery of Dexamethasone and green tea polyphenols using electrospun ultrafine fibers for effective treatment of keloid. Pharm Res 31:1632–1643. https://doi.org/10.1007/s11095-013-1266-2

Lin N, Dufresne A (2014) Nanocellulose in biomedicine: current status and future prospect. Eur Polym J 59:302–325. https://doi.org/10.1016/j.eurpolymj.2014.07.025

Liu J, Chinga-Carrasco G, Cheng F, Xu W, Willför S, Syverud K, Xu Ch (2016) Hemicellulose-reinforced nanocellulose hydrogels for wound healing application. Cellulose 23:3129–3143. https://doi.org/10.1007/s10570-016-1038-3

Mendoza-Milla C, Machuca Rodríguez C, Córdova Alarcón E, Estrada Bernal A, Toledo-Cuevas EM, Martínez Martínez E, Zentella Dehesa A (2005) NF-κB activation but not PI3 K/Akt is required for dexamethasone dependent protection against TNF-α cytotoxicity in L929 cells. FEBS Lett 579:3947–3952. https://doi.org/10.1016/j.febslet.2005.05.081

Messner M, Loftsson T (2010) Solubility and permeability of steroids in water in the presence of potassium halides. Pharmazie 65:83–85. https://doi.org/10.1691/ph.2010.9211

Moritz S, Wiegand C, Wesarg F, Hessler N, Muller FA, Kralisch D, Hipler UC, Fischer D (2014) Active wound dressings based on bacterial nanocellulose as drug delivery system for octenidine. Int J Pharm 471:45–55. https://doi.org/10.1016/j.ijpharm.2014.04.062

Napavichayanun S, Yamdech R, Aramwit P (2016) The safety and efficacy of bacterial nanocellulose wound dressing incorporating sericin and polyhexamethylene biguanide: in vitro, in vivo and clinical studies. Arch Dermatol Res 308:123–132. https://doi.org/10.1007/s00403-016-1621-3

Nieuwenhuis B, Luth A, Kleuser B (2010) Dexamethasone protects human fibroblasts from apoptosis via an S1P3-receptor subtype dependent activation of PKB/Akt and BclXL. Pharmacol Res 61:449–459. https://doi.org/10.1016/j.phrs.2009.12.005

Papadopoulou V, Kosmidis K, Vachou M, Macheras P (2006) On the use of the Weibull function for the discernment of drug release mechanisms. Int J Pharm 309:44–50. https://doi.org/10.1016/j.ijpharm.2005.10.044

Raghavendra Reddy Y, Srinath N, Nandakumar H, Rajini Kanth M (2012) Role of collagen impregnated with dexamethasone and placentrix in patients with oral submucous

fibrosis. J Maxillofacc Oral Surg 11:166–170. https://doi.org/10.1007/s12663-011-0274-1

Ren H, Liang D, Jiang X, Tang J, Cui J, Wei Q, Zhang S, Yao Z, Shen G, Lin S (2015) Variance of spinal osteoporosis induced by dexamethasone and methylprednisolone and its associated mechanism. Steroids 102:65–75. https://doi.org/10.1016/j.steroids.2015.07.006

Spaic M, Small DP, Cook JR, Wan W (2014) Characterization of anionic and cationic functionalized bacterial cellulose nanofibres for controlled release applications. Cellulose 21:1529–1540. https://doi.org/10.1007/s10570-014-0174-x

Ul-Islam M, Khan T, Khattak WA, Park JK (2013) Bacterial cellulose-MMTs nanoreinforced composite films: novel wound dressing material with antibacterial properties. Cellulose 20:589–596. https://doi.org/10.1007/s10570-012-9849-3

Vardy J, Chiew KS, Galica J, Pondand GR, Tannock IF (2006) Side effects associated with the use of dexamethasone for prophylaxis of delayed emesis after moderately emetogenic chemotherapy Br. J Cancer 94:1011–1015. https://doi.org/10.1038/sj.bjc.6603048

Wang AS, Armstrong EJ, Armstrong AW (2013) Corticosteroids and wound healing: clinical considerations in the perioperative period. Am J Surg 206:410–417. https://doi.org/10.1016/j.amjsurg.2012.11.018

Weijtens O, Schoemaker RC, Romijn FP, Cohen AF, Lentjes EG, van Meurs JC (2002) Intraocular penetration and systemic absorption after topical application of dexamethasone disodium phosphate. Ophthalmology 109:1887–1981. https://doi.org/10.1016/S0161-6420(02)01176-4

White ES, Mantovani AR (2013) Inflammation, wound repair, and fibrosis: reassessing the spectrum of tissue injury and resolution. J Pathol 229:141–144. https://doi.org/10.1002/path.4126

Wu WS, Wang F-S, Yang KD, Huang CC, Kuo YR (2006) Dexamethasone induction of keloid regression through effective suppression of VEGF Expression and keloid fibroblast proliferation. J Investig Dermatol 126:1264–1271. https://doi.org/10.1038/sj.jid.5700274

Zakkar M, le Luong A, Chaudhury H, Ruud O, Punjabi PP, Anderson JR, Mullholand JW, Clements AT, Krams R, Foin N, Athanasiou T, Leen EL, Mason JC, Haskard DO, Evans PC (2011) Dexamethasone arterializes venous endothelial cells by inducing mitogen-activated protein kinase phosphatase-1: a novel antiinflammatory treatment for vein grafts? Circulation 123:524–532. https://doi.org/10.1161/CIRCULATIONAHA.110.979542

Zhang B, Molino PJ, Harris AR, Yue Z, Moulton SE, Wallace GG (2016) Conductive and protein resistant polypyrrole films for dexamethasone delivery. J Mater Chem B 4:2570–2577. https://doi.org/10.1039/c5tb00574d